Origin of slow, heavy residues observed in dissipative ^{197}Au+^{86}Kr collisions at $E/A=35$ MeV

W. Skulski,* B. Djerroud, D. K. Agnihotri, S. P. Baldwin, J. Tõke, X. Zhao, and W. U. Schröder
Department of Chemistry and NSRL, University of Rochester, Rochester, New York 14627

L. G. Sobotka, R. J. Charity, J. Dempsey, and D. G. Sarantites
Department of Chemistry, Washington University, St. Louis, Missouri 63130

B. Lott
GANIL (IN2P3–CNRS, DSM–CEA), BP 5027, Caen 14021, France

W. Loveland
Department of Chemistry, Oregon State University, Corvallis, Oregon 97331

K. Aleklett
Studsvik Neutron Research Laboratory, Uppsala University, S–611 82 Nyköping, Sweden

(Received 18 March 1996)

An exclusive measurement of slow, massive residues from the ^{197}Au+^{86}Kr reaction at E/A=35 MeV has been performed in coincidence with projectile-like fragments, neutrons, as well as light- and intermediate-mass charged products. The highly efficient (double 4π) detector setup used included the University of Rochester SuperBall neutron detector and the Washington University Microball. The observed large yield of slow, massive residues shows characteristics consistent with a production scenario similar to that of binary dissipative collisions. The residues result from the statistical decay of primary targetlike fragments, produced even in the most dissipative collisions identified in the present experiment. [S0556-2813(96)50906-4]

PACS number(s): 25.70.Lm, 25.70.Pq

Heavy-ion reaction studies at intermediate bombarding energies [1] of several tens of MeV per nucleon have revealed the onset of various phenomena not encountered at lower bombarding energies [2]. At the same time, evidence has been mounting for the dominance of processes reminiscent of binary dissipative collisions, at least at the lower boundary of the Fermi-energy domain and not too asymmetric systems. Here, most of the reaction cross section is associated [3,4] with the production of primary projectilelike and targetlike fragments, PLF and TLF, respectively, which subsequently decay statistically.

Expecting this dissipative-collision scenario to be of general validity for intermediate-energy heavy-ion reactions, one is tempted to identify much of the yield of slow ($E/A\approx 0.1$–0.5 MeV), heavy residues (HR), observed [5] in a recent radiochemical study of the reaction ^{197}Au+^{86}Kr over a broad angular range, with the remnants of primary TLF's. HR's are defined here to have masses in excess of $\approx 1/3$ of the target mass. The case can be made easily for HR's emitted close to the TLF grazing angle. However, previous studies did not answer the question concerning the origin of slow HR's associated with large cross section measured at forward angles. A number of possible reaction mechanisms have been considered [5–10], such as fusion-like, fast fission, fragmentation, spallation, and dissipative collisions. Retardation of fission was also considered [11], which could constitute an interesting continuation of trends observed [12] in studies of prescission particle emission in heavy-ion-induced fission at lower energies. Since determination of the reaction mechanism requires information on correlations between the HR yields and other reaction observables, an exclusive measurement of HR's has been performed in the work presented here. HR's were measured in coincidence with all types of charged reaction products, as well as with neutrons. In particular, a measurement of kinematical coincidences between HR's and PLF's provided crucial and unambiguous information on the origin of slow, heavy residues.

The experiment was performed at the K1200 cyclotron of the National Superconducting Cyclotron Laboratory at Michigan State University. A 35 MeV/nucleon ^{86}Kr beam bombarded a 0.3 mg/cm^2 thick ^{197}Au target. The experimental setup included the Rochester SuperBall neutron detector, the Washington University Microball charged-particle detector array, and a number of silicon detectors. Elastically scattered projectiles and PLF's were measured with two position-sensitive Si-detector telescopes covering the angular range between $\theta=-2°$ and $\theta=-8°$. Both telescopes provided atomic-number resolution in the range of $1<Z<38$. Normalization of the elastic-scattering yield to the Rutherford cross section at forward angles provided a cross section scale for this work.

Slow, heavy reaction products, along with light charged particles (LCP) and intermediate-mass fragments (IMF), were measured with three 40×61.5 mm^2, 0.3 mm thick multistrip silicon detectors, covering the angular range between $\theta=+9°$ and $\theta=+46.5°$, on the side of the beam opposite to the PLF telescopes. A coarse time-of-flight (TOF) measure-

*On leave of absence from the Heavy Ion Laboratory, Warsaw University, Poland.

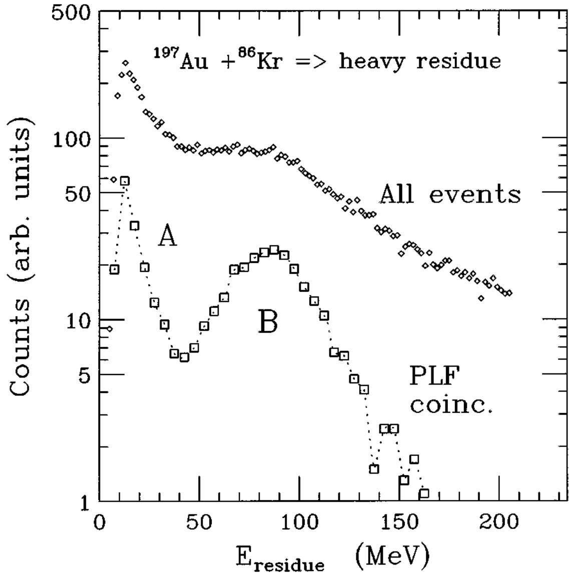

FIG. 1. Energy spectra of heavy residues observed in the angular range between 9° and 46.5° in ''singles'' mode (diamonds) and in coincidence with PLF's with $Z_{PLF}>25$ (squares). The low-energy peak is due to the detection threshold.

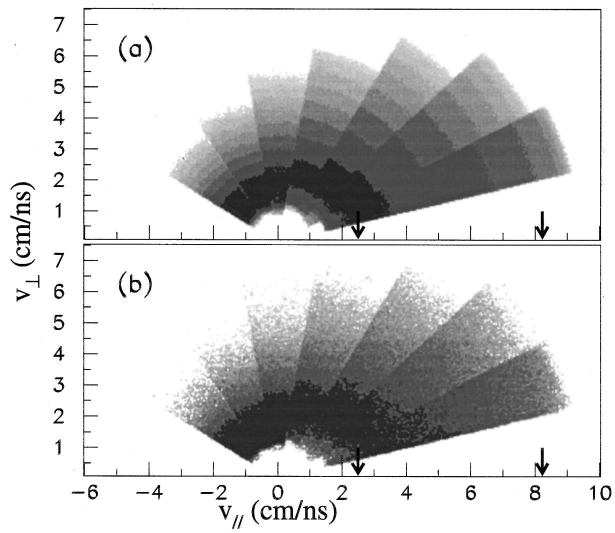

FIG. 2. Emission patterns of α particles in a Galilei-invariant representation of the yield vs the velocity components $v_{\parallel}$ and $v_{\perp}$. Panel (a): all events. Panel (b): events in coincidence with a heavy fragment detected at angles between 9° and 46.5° in lab. The center-of-mass and beam velocities are marked with arrows.

ment was performed, where these strip detectors provided the stop signals, while start signals were derived from either the accelerator RF signal or a 17 mg/cm^2 thick plastic scintillation detector close to the target. The latter detector, which measured PLF's in coincidence with HR's, introduced a threshold on the PLF atomic number at $Z_{PLF}\approx 25$ into the corresponding TOF measurement. Both TOF measurements had sufficient accuracy to distinguish unambiguously between HR's, LCP's, and IMF's, when combined with the appropriate energy information. Product identification was possible for HR's with energies larger than $E_{HR}\approx 15$ MeV, accounting for pulse-height defect. Energy calibrations of the Si detectors were achieved using either radioactive sources, elastically scattered projectiles, or the information on maximum energy deposits (''punch-through energies'') for various charged products.

Neutrons were measured with the University of Rochester SuperBall neutron detector enclosing the scattering chamber in 4π geometry. The SuperBall was filled with 16.3 m^3 of gadolinium-loaded liquid scintillator (National Diagnostics ND-309), viewed by 52 Thorn-EMI 9390KB07 5 in. photomultipliers. The detector measured the multiplicity of neutrons and provided, via the prompt light output signal, also a measure of the total kinetic neutron energy. LCP's and IMF's were measured with the Washington University Microball, reconfigured here to allow operation of the Si strip detectors and telescopes. The Microball covered 95% of the full solid angle, in the angular range $14°<\theta<171°$. It resolved elements with $Z<5$ and, in addition, the three hydrogen isotopes. During the experiment, the data acquisition system accepted data, whenever either a Si detector, the SuperBall, or the Microball registered an event.

Experimental results are presented in Figs. 1–3. Figure 1 exhibits angle-integrated, apparent HR energy spectra, not corrected for the pulse-height defect. These spectra were measured with the strip detectors, either in singles mode (diamonds), or in coincidence (squares) with PLF's ($Z_{PLF}>25$) detected with the scintillation detector. The HR singles yield is significant, representing an integrated cross section of $\sigma=(1.0\pm 0.1)$ b, approximately 20% of the total reaction cross section. The two energy spectra of Fig. 1 look very similar: a Gaussian (B), centered at an apparent energy of $E\approx 90$ MeV, is superimposed on a broad distribution (A), which decreases in intensity continuously, from the detection threshold, with increasing HR energy. The intensity ratio of the components in the measured inclusive spectrum amounts to $A{:}B\approx 0.7$, which could be lower than the actual ratio by $\approx 30\%$ due to detection thresholds. The Gaussian component, as well as the rise toward low energies, are somewhat better defined in the exclusive spectrum, as can be expected, owing to the limits in HR recoil angle and energy imposed by the kinematical coincidence condition. Since these massive HR's illustrated in Fig. 1 (bottom) appear in kinematic coincidence with PLF's, they are clearly remnants of the primary TLF's.

An identification of HR's with the remnants of TLF's, produced in dissipative collisions, can rigorously only be made for that subset of the HR data, for which a coincident PLF has actually been detected. However, this conclusion appears to remain true for the entire set of HR events measured in the present experiment. This is obvious from inspection of Galilei-invariant velocity distributions of α particles and other LCP's emitted in the reaction. In Fig. 2, the measured yields of α particles are shown as contour diagrams, plotted vs α particle laboratory velocity components parallel and perpendicular to the beam, respectively. The data in Fig. 2(a) include all events, while the plot of Fig. 2(b) represents only coincidences with massive HR's. The arrows indicate the velocities of the beam projectiles and of the center of mass, respectively.

The approximately semicircular intensity pattern (''Coulomb ring'') of the velocity plots shown in Fig. 2 identifies clearly a slow-moving, massive, evaporative source as the dominant origin of the α particles measured with the Mi-

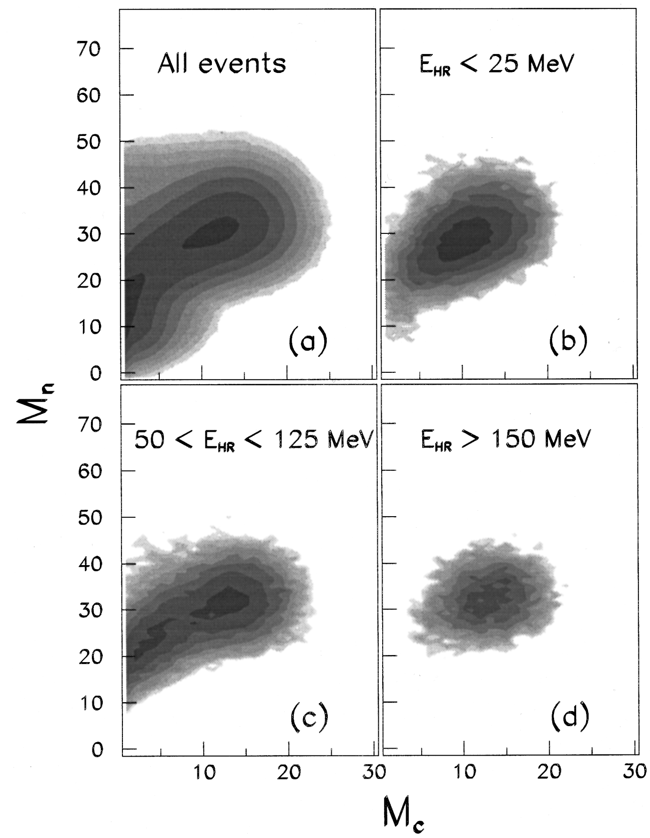

FIG. 3. Logarithmic contour plots of the joint multiplicity distribution of neutrons (m_n) and charged particles (m_c), as measured (a) for all events with $m_c > 1$; and in coincidence with HR's in the following ranges of energy: (b) $E_{\mathrm{HR}} < 25$ MeV (''A'' in Fig. 1); (c) $50 < E_{\mathrm{HR}} < 125$ MeV (''B'' in Fig. 1); and (d) $E_{\mathrm{HR}} > 150$ MeV.

croball. The velocity of this emitter, defined by the center of the ''Coulomb ring,'' is significantly smaller than that of the center of mass. It increases somewhat with increasing particle multiplicity, consistent with a dissipative reaction scenario. Consequently, this emitter is very different from a composite nucleus that could have been formed in the ^{197}Au+^{86}Kr reaction. This is not surprising for the semi-inclusive distribution of Fig. 2(a), where most of the α particles have presumably been emitted sequentially from TLF's produced in the peripheral to midcentral collisions that dominate this data set. It has also been verified that, even if the heavy primary TLF undergoes fission, the associated α-particle emission pattern is determined by prescission emission [12]. Therefore, this pattern still reflects the properties of the TLF, rather than those of the fission fragments. The Coulomb ring pattern associated with a similar emission process involving the PLF, is more compact and centered at a higher velocity than that for the TLF. Consequently, the former pattern is largely missed by the Microball LCP detectors, except for a slight enhancement in intensity, visible in Fig. 2(a) at the most forward angles.

For similar reasons, the invariant α particle velocity distribution of Fig. 2(b), measured in coincidence with slow, massive HR's, is consistent with emission from just these HR's. Apart from a weak component due to the corresponding fast PLF emitter, there is no positive evidence for any additional source of α particles, specifically not for one that moves with the velocity of the center of mass. Therefore, it appears justified to identify the observed HR's with the remnants of TLF's produced in dissipative collisions also in those cases, where no PLF has been detected in coincidence. Another piece of evidence supporting this conclusion is provided by the magnitude of the HR cross section [$\sigma_{\mathrm{HR}} = (1.0 \pm 0.1)$ b], which is consistent with that of the TLF's [$\sigma_{\mathrm{TLF}} = (1.6 \pm 0.2)$ b], expected within the angular range of the residue detectors. This latter cross section was deduced from the angular distribution of the PLF reaction partners also measured in this experiment. The difference between the value of σ_{HR} obtained in this work and the one measured with radiochemical methods [5,13], $\sigma_{\mathrm{HR}} = (3.0 \pm 0.4)$ b, is attributed to detection thresholds in the present experiment.

Since the HR's have been identified with remnants of TLF collision partners, one is able to interpret their two-component energy spectrum illustrated in Fig. 1. From the angle-energy distribution of PLF's (the Wilczyński plot) establishing [14,15] the binary dissipative character of the ^{197}Au+^{86}Kr reaction, it is known that the cross section decreases with increasing momentum transfer to the corresponding TLF's. The resulting broad TLF energy distribution is consistent with only one of the spectral components (A) seen in Fig. 1, suggesting that the latter actually represents the TLF evaporation residues (TLF-ER). Furthermore, it turns out that the average energy of the Gaussian component (B), centered at an energy of $E \approx 90$ MeV, coincides with that measured for ^{252}Cf fission fragments during off-line calibration. Therefore, component B is identified with fragments (TLF-FF) resulting from fission of the TLF's. Interestingly, these latter TLF's are associated with less dissipative collisions than those leading to TLF-ER's. This conclusion is based on the multiplicity correlations (m_c versus m_n), which are different for TLF-FF's and for TLF-ER's, and on the different velocities of the coincident PLF's [14]. Figure 3 presents the inclusive joint multiplicity distribution $P(m_c, m_n)$, as well as several conditional distributions, in the form of contour diagrams. The neutron multiplicity has been corrected for background, but neither the quantity m_n nor m_c have been corrected for detection efficiency or solid angle. The intensity pattern depicted in Fig. 3(a) illustrates the evolution of energy dissipation with impact parameter, assuming that there is an approximately monotonic relation between these two quantities [2]. A continuous probability (cross section) ridge extends from the region corresponding to low degrees of dissipation (peripheral collisions) near the origin of the plot, to a broad bump at $(m_c, m_n) \approx (15,30)$, associated with highly dissipative, i.e., fairly central, collisions. This bump corresponds to a dissipated energy of approximately 1 GeV, as obtained from a ''moving-source'' analysis of the backward-angle particle emission patterns. It is also significant to note, that only the exponentially decreasing tail of the multiplicity distribution extends to the domain of complete damping in a binary collision, $m_c > 35$ and $m_n > 60$, but does not reach to higher multiplicities expected for the complete fusion process. Based on this observation, it does not seem likely that complete fusion constitutes a significant fraction of the total reaction cross section, in agreement with earlier conclusions drawn from Fig. 2.

Figure 3(b) shows the multiplicity distribution measured in coincidence with the low-energy ($E_{\mathrm{HR}} < 25$ MeV) evaporation residues TLF-ER, i.e., component *A* in Fig. 1. This HR component is indeed associated with high degrees of dissipation, albeit not the highest ones, as demonstrated by the location of the maximum of the distribution at $(m_c, m_n) \approx (12{,}25)$. The multiplicity distribution shown in Fig. 3(c) is measured in coincidence with HR's in the region of energies 50 MeV $< E_{\mathrm{HR}} < 125$ MeV, dominated by the Gaussian TLF-FF component *B*, but containing also significant contribution from the TLF-ER component *A* (see Fig. 1). Consequently, the multiplicity distribution of Fig. 3(c) also shows two components representing high and intermediate degrees of dissipation, respectively. In fact, using the requirement of a coincidence with PLF's, the lower multiplicity component was identified with that of lower dissipation. The separation between the components is not as good as that seen in Fig. 1 because of the inherent width of the multiplicity distributions. Finally, the distribution in Fig. 3(d) corresponds to $E_{\mathrm{HR}} > 150$ MeV, i.e., the high-energy tail of the HR-ER spectrum. Consistent with the kinematics of dissipative collisions, the distribution of Fig. 3(d) is indicative of the highest degrees of dissipation observed in this work. One should note, that significant contamination due to quasielastic collisions is not observed in any of the Figs. 3(b), 3(c), or 3(d).

The sequence of joint multiplicity distributions displayed in Fig. 3 shows that TLF-ER's arise from more dissipative collisions than the TLF-FF component. A decomposition of the multiplicity distribution shown in Fig. 3(c), which contains both components, yields an intensity ratio of TLF-ER:TLF-FF $\approx 0.8{:}1$, in good agreement with the decomposition of the HR energy spectrum of Fig. 1, discussed previously. This agreement corroborates the earlier conclusion, that the more dissipative ^{197}Au+^{86}Kr collisions lead to TLF-evaporation residues, rather than to TLF fission fragments.

In summary, the present work has demonstrated that the slow, massive residues, observed in ^{197}Au+^{86}Kr collisions at $E/A = 35$ MeV and angles between 9° and 46.5°, are remnants of the primary TLF's emitted in highly dissipative collisions, a possibility considered previously also by other workers [6]. The more dissipative collisions appear to lead to evaporation residues, while slightly less dissipative reactions favor a fission decay of the primary TLF's. This effect could be the result of the emission of increased numbers of neutrons and charged products from the system, leading to less fissile TLF's at higher dissipation.

Within experimental uncertainties, the detected HR cross section is consistent with the cross section deduced for massive TLF's emitted into the angular range covered by the HR detectors, as deduced from the measured PLF distribution. Consistent with the absence of complete energy damping, no positive evidence has been found in the present data for products of a fusionlike reaction, reported by others [16]. However, a relatively small cross section for such processes cannot be excluded, should they be associated with thermal excitation energies significantly lower than the initially available kinetic energy of relative motion, and with HR emission forward of $\theta < 9°$ in this reaction. Based on present reaction theories such as BUU, much larger cross sections for fusion or fusionlike processes are expected for an asymmetric reaction at intermediate energies, than those consistent with present work. The most remarkable finding of the present work is the fact that the TLF's survive the collision stage as massive fragments, before decaying statistically via evaporation or sequential fission. This unexpected stability of nuclei is observed even for collisions associated with the highest dissipated energies identified in this work (≈ 1 GeV), i.e., presumably for rather central collisions. These findings provide new and important challenges to the present understanding of dynamical nuclear response and nuclear structure in intermediate-energy heavy-ion collisions.

The authors wish to express their appreciation of the kind hospitality extended to them at the NSCL and are grateful to the K1200 operations crew, in particular to Jeffrey Stetson, for an efficient operation of accelerator and beam transport system. This work was supported by the U.S. Department of Energy under Grant Nos. DE-FG02-88ER40414 and DE-FG02-87ER40316.

[1] C.K. Gelbke and D.H. Boal, Prog. Part. Nucl. Phys. **19**, 33 (1987), and references therein.
[2] W.U. Schröder and J.R. Huizenga, in *Treatise in Heavy-Ion Science*, edited by D.A. Bromley (Plenum Press, New York and London, 1984), Vol. 2, p. 113, and references therein.
[3] B. Lott *et al.*, Phys. Rev. Lett. **68**, 3141 (1992).
[4] S. P. Baldwin *et al.*, in *Advances in Nuclear Dynamics,* edited by B. Back, W. Bauer, and J. Harris (World Scientific, Singapore, 1993), p. 36; S. P. Baldwin *et al.*, Phys. Rev. Lett. **74**, 1299 (1995).
[5] K. Aleklett *et al.*, Phys. Lett. B **236**, 404 (1990); W. Loveland *et al.*, Phys. Rev. C **41**, 973 (1990).
[6] E. Schwinn *et al.*, Nucl. Phys. **A568**, 169 (1994).
[7] E.C. Pollacco *et al.*, Nucl. Phys. **A583**, 441 (1995).
[8] D. Utley *et al.*, Phys. Rev. C **49**, R1737 (1994).
[9] A.A. Sonzogni *et al.*, Phys. Rev. C **53**, 243 (1996).
[10] K. Hanold *et al.*, Phys. Rev. C **52**, 1462 (1995).
[11] R. Yanez *et al.*, Phys. Rev. C **52**, 203 (1995).
[12] D. Hilscher and H. Rossner, Ann. Phys. (Paris) **17**, 471 (1992).
[13] W. Loveland (private communication).
[14] W. Skulski *et al.*, in *Advances in Nuclear Dynamics,* edited by W. Bauer (World Scientific, Singapore, 1995).
[15] B. Djerroud *et al.* (unpublished).
[16] J.B. Natowitz, in Proceedings of the American Chemical Society Nuclear Chemistry Award Symposium, Anaheim, CA, 1995 (unpublished).